

TURBULENCE MEASUREMENTS IN A QUASI-TWO DIMENSIONAL JET IN A SLOT CHANNEL

Artur V. Bilsky, Vladimir M. Dulin, Dmitriy M. Markovich, Maxim V. Shestakov

Institute of Thermophysics,

Siberian Branch of Russian Academy of Sciences

Ak. Lavrentyev ave. 1, Novosibirsk, 630090, Russia

bilsky@itp.nsc.ru, vmd@itp.nsc.ru, dmark@itp.nsc.ru, mvsh@itp.nsc.ru

ABSTRACT

Turbulent structure of a jet spreading in a narrow channel is studied experimentally by using PIV. A wide range of the Reynolds number, defined on the basis of the mean flow rate velocity and a hydraulic diameter of rectangular nozzle, was covered (from 500 up to 50,000). External low-amplitude forcing of inlet velocity was performed to study the influence of large-scale vortices developing in the jet shear layer on the flow structure. On the basis of the special measurements with a high spatial resolution the one-dimensional spatial spectra were calculated for initial and far regions of the jet. Two typical spectrum slopes were clearly observed: -3 slope in the low wave number region and -1 slope in the high wavenumber region.

Spatial distributions of the statistical moments of velocity fluctuations up to the third-order were obtained. It is demonstrated, that the forcing affects significantly the flows with low and moderate Re leading to greater values of the moments in the near-nozzle region of the jet.

For the case, corresponding to $Re = 20,000$, terms of the mean momentum and turbulent kinetic energy (TKE) budget equations were estimated for a far region of the jet. For the axial mean momentum, convection and mean pressure gradient mainly contribute to the balance equation, while for TKE the effect of the convection was found to be rather small.

INTRODUCTION

Quasi-2D turbulent jet flows are widely spread in nature and industry. Geophysical turbulence, where two-dimensionality in relatively thin layers occurs due to earth rotation and density stratification, contains horizontal mixing layers developing under the conditions where the third velocity component is rather suppressed relatively to other directions. Many practical applications and developing devices assume the jets to be spreading in narrow gaps: geothermal engineering, modern mini-channel chemical processors, cooling systems, etc. Modeling of filtration processes and development of optimal methods for raw oil extraction also require comprehensive information on structure of such flows.

Jet flows in slot channels have a number of peculiarities making them essentially different from free jets and channel flows. Development of Kelvin-Helmholtz vortices is accompanied in this case by a strong influence of wall friction that leads to the existence of a variety of fundamentally different regimes: from classical Hele-Shaw regimes up to developed turbulent flows that manifest some features of 2D turbulence.

Now there is a lack of the experimental studies of 2D turbulence, that is partially due to the experimental difficulties of a reaching two-dimensionality of the flow.

The list of articles is restricted by a few works on thin soap film experiments, MHD turbulence etc. As for jets spreading in narrow gaps the following works need to be mentioned: Gorin et al. (1998) performed some LDA measurements for turbulent jet in a slot channel; Chu and Baines (1989) studied buoyant turbulent jet between confined walls; Pesci et al. (2003) described experimentally and developed some theoretical scenario of Kelvin-Helmholtz instability development in a system with low- Re jet spreading in a Hele-Shaw cell. The data on the analysis of different flow regimes and comprehensive information on turbulent characteristics for the slot jets are absent in the literature. The present work is devoted to the experimental study of a jet spreading in a narrow slot for the wide range of Reynolds numbers.

EXPERIMENTAL SETUP AND APPARATUS

The slot channel (see Figure 1) was formed by two parallel rectangular optical glass sheets $640 \times 480 \text{ mm}^2$ placed at a distance of $h = 2.4 \text{ mm}$ from each other. The width of a non-profiled nozzle was equal to $d = 24 \text{ mm}$. A measurement section represented the part of a hydraulical contour, consisting of system of pumps, flow-meters and a temperature stabilizing device. A constant header tank was used for flow rate stabilization and to suppress external vibrations. Water temperature was maintained constant 26°C with variations of $\pm 0.5^\circ\text{C}$.

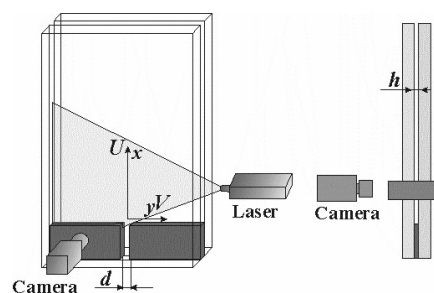


Figure 1: Measurement section, coordinate system, and apparatus arrangement.

During the experiments the Reynolds number derived on the mean flow rate velocity U_0 and doubled depth of the slot $2h$ was varied from $Re = 2U_0h/\nu = 500$ to 50,000. In order to study the dynamics of large scale vortices in confined shear layer of the jets, an external low-amplitude periodical forcing was applied with Strouhal number $St = fU_0/d = 0.5$, where f is the forcing frequency.

Non-intrusive method for flows diagnostics, Particle Image Velocimetry, was used for velocity measurements. Measurements were performed in the plane parallel to the

glass sheets in central cross-section of the slot. For reaching high spatial resolution, the whole measurement area was separated into three zones (Figure 1, b), where the measurements were performed independently. The jet structure was investigated in the area located from the nozzle exit and up to the distance of $9d$ in the streamwise direction. A "PIVIT" PIV system, consisting of a CCD camera, a double-cavity Nd:YAG pulsed laser and a synchronizing device, was used for velocity fields measurements. The number of PIV images obtained for each measurement zone was equal to 3,000. The images were processed by "ActualFlow" software using iterative cross-correlation algorithm with an image deformation (CWD). Measured ensemble of instant velocity fields allowed calculation of spatial spectra and one-point statistical moments. In order to provide accurate calculation of statistical moments, "false" vectors filtration was performed by using procedure reported by Heinz et al. (2004).

RESULTS AND DISCUSSION

Reynolds number and forcing effect

The slot jet structure was found to be strongly sensitive to the Reynolds number that generally corresponds to the previous works (Nakoryakov et al., 1991). Variations of the normalized centerline jet velocity U_s along the jet axis are presented in Figure 2 for the different Reynolds numbers. The data obtained are compared with results of LDA measurements (shown as symbols in Figure 2) for the similar experimental assembly by Nakoryakov et al. (1991).

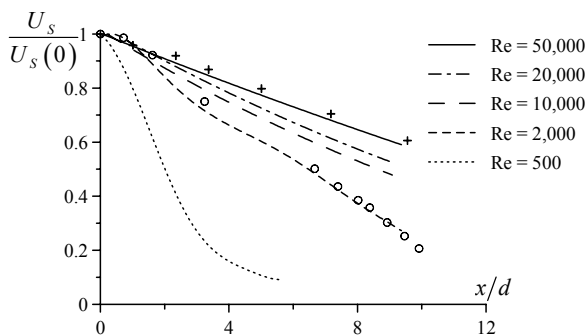


Figure 2: Axial mean velocity decay along the jet axis.

It was found that for the flow with $Re = 500$, intensity of velocity fluctuations are small and this case is further considered as laminar. Spatial distributions of the statistical moments for the flows with $Re = 10,000$, $20,000$ and $50,000$ are quite similar in shape and the magnitudes of the moments grow with Re . The case with $Re = 2,000$ significantly differs from the cases mentioned above and in the present study is considered as transitional.

Spatial distributions of the second-order moment are presented in Figures 3 and 4 for the slot jets with various Reynolds numbers. It was revealed that for the transitional case, maximum values of the normalized $\langle u^2 \rangle$, reached in the mixing layer in the vicinity of the nozzle exit, are about five times greater than for the cases of $Re \geq 10,000$. The effect of external forcing is shown in Figure 5. External periodical forcing leads to a strong changing in the jet structure at low and moderate Reynolds numbers ($2,000$ and $10,000$) and to very high values of the turbulent kinetic energy in the initial region of the jets. During the forcing, large-scale vortices in the initial region were amplified resonantly that is reflected

by distributions of second- and third-order statistical moments (examples of the third-order moments are shown in Figure 9). However, at far downstream edge of the measurement area, more rapid decay of the moments for the forced jets is observed. For the high Reynolds numbers $Re = 20,000$ and $50,000$, contrary, the flow structure was almost insensitive to the external forcing.

By using experimental data from additional high resolution PIV measurements in certain regions of the flow at $Re = 20,000$, one-dimensional spatial spectra were calculated in the streamwise direction for both forced and unforced flow conditions. The maximum wavenumber of plotted spectra corresponds to π/Δ value, where Δ is the final interrogation area size for CWD algorithm. In Figure 6a and b one-dimensional spectra are presented for ($x/d = 0.1-1.2$, $y/d = 0.5$) and ($x/d = 9.5-10.6$, $y/d = 0.9$) regions of the jet. In the vicinity of the nozzle edge (Figure 6a) the spectra reflect growth of periodical structures intensity (maximum appears at a corresponding wavenumber). Two typical slopes -3 and -1 are observed, which characterize quasi two-dimensionality of the flow. With increasing of streamwise distance, the maxima in spectral distributions disappear and -3 slope becomes more pronounced. Previously, slopes -3 and -1 were also observed by Drakos et al. (1992) for the plane jet spreading in bounded fluid layer with significantly lesser values of Re and aspect ratio d/h . The authors reported that for this flow regime the large-scale vortex structures develop in the jet mixing layer and grow downstream due to their pairing.

Figure 7 shows evolution of the mean streamwise velocity with x/d and demonstrates effect of the forcing. With increase of Re , the jet centerline velocity decay and the jet spreading rate slightly decreases. For the cases with $Re \geq 10,000$, the effect of the forcing on the mean flow velocity is barely visible, while for the transitional case with $Re = 2,000$, the forcing leads to a slightly faster decay of the axial velocity.

Profiles of the spanwise component $\langle v^2 \rangle$ of turbulent kinetic energy are presented in Figure 8. For unforced cases with $Re = 10,000$ and $50,000$, profiles of $\langle v^2 \rangle$ have similar shape and in the latter case magnitude of $\langle v^2 \rangle$ is greater. The highest magnitudes of the normalized spanwise component of turbulent kinetic energy are observed to be at the initial region $x/d \leq 4$ of the transitional flow ($Re = 2,000$). For both cases with $Re = 10,000$ and $2,000$ the forcing leads to significantly greater values of the turbulent kinetic energy in the vicinity of the nozzle (also see Figure 5) and to a faster decay of its magnitude.

As an example, distributions of the third-order moment $\langle u^3 \rangle$, corresponding to the axial flux of the axial component of the turbulent kinetic energy, are presented in Figure 9 for the same flows and cross-sections as in Figures 7 and 8. Moment $\langle u^3 \rangle$ was selected for presentation as having a large magnitude peculiarity for $Re = 2,000$ case at $x/d = 2$ cross-section, where high values of $\langle u^2 \rangle$ were also observed (see Figure 3a). From Figure 9a it can be seen, that application of the external forcing strongly suppresses $\langle u^3 \rangle$ in this region, similarly to $\langle v^2 \rangle$. For the flows with $Re \geq 10,000$, $\langle u^3 \rangle$ takes on mainly negative values in the inner region of the mixing layer of the jet and positive values in the outer layer. For $Re = 10,000$ case, the forcing gives rather non-uniform effect: it leads to increase of $\langle u^3 \rangle$ magnitude in the area of negative values and to decrease it in the area of positive values.

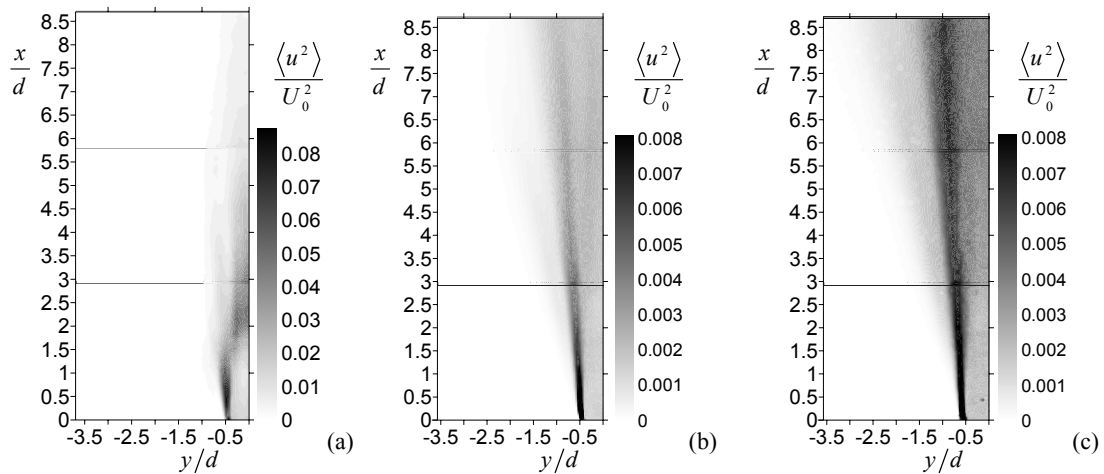


Figure 3: Spatial distributions of the normalized streamwise component of turbulent kinetic energy for unforced slot jets. (a) $Re = 2,000$; (b) $Re = 10,000$ (c) $Re = 50,000$

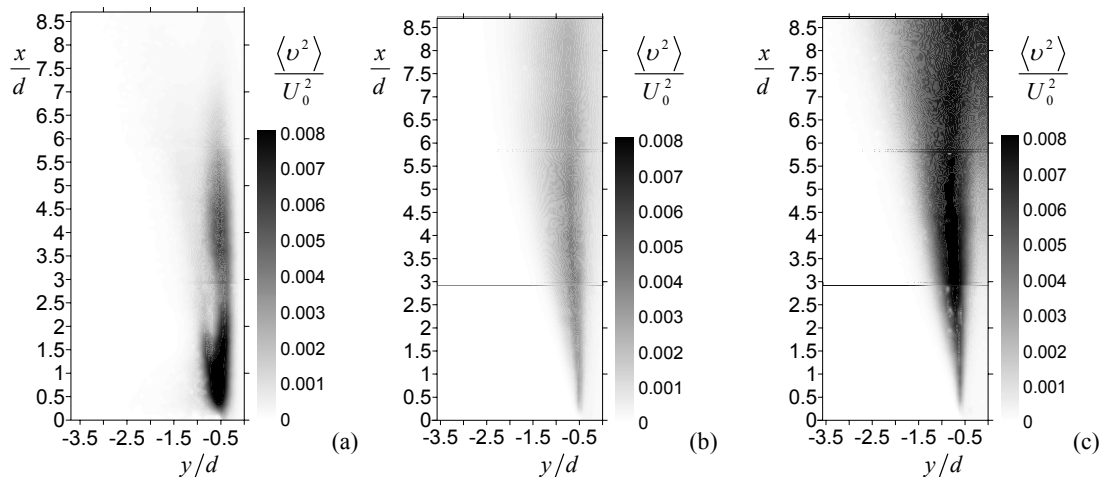


Figure 4: Spatial distributions of the normalized spanwise component of turbulent kinetic energy for unforced slot jets. (a) $Re = 2,000$; (b) $Re = 10,000$ (c) $Re = 50,000$

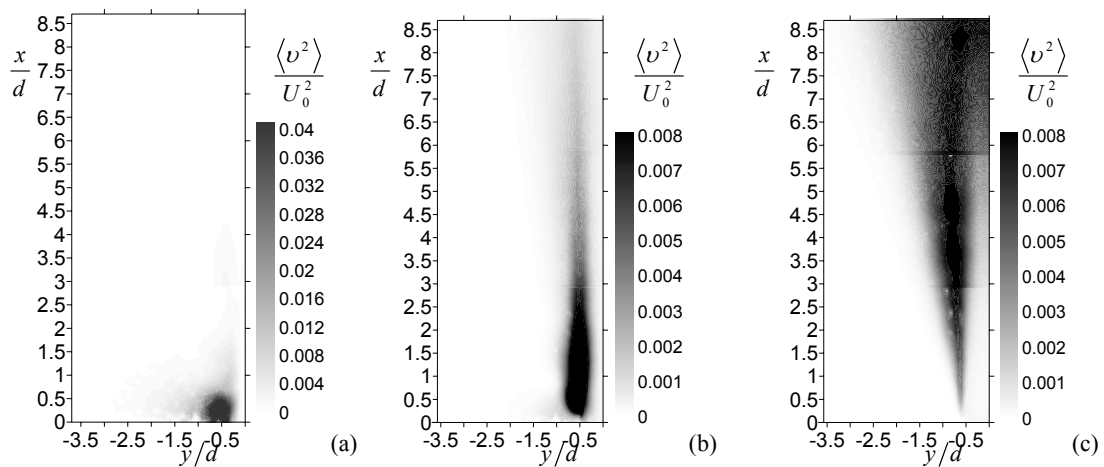


Figure 5: Spatial distributions of the normalized spanwise component of turbulent kinetic energy for forced slot jets. (a) $Re = 2,000$; (b) $Re = 10,000$ (c) $Re = 50,000$

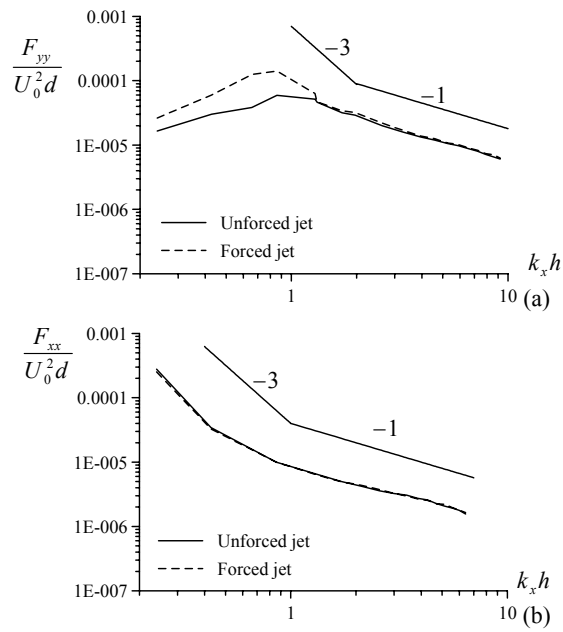


Figure 6: One-dimensional spectra for slot jet at $Re = 20,000$ at $x/d = 6$. (a) Spectrum of the spanwise velocity fluctuations, initial region of the jet (b) Spectrum of the streamwise velocity fluctuations, far region of the jet.

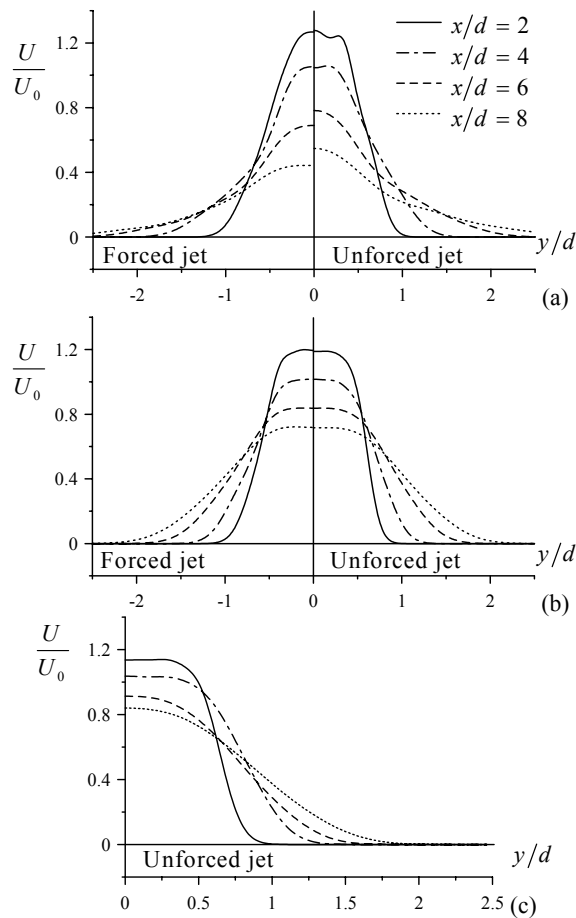


Figure 7: Streamwise mean velocity distributions at various cross-sections of slot jet. (a) $Re = 2,000$; (b) $Re = 10,000$; (c) $Re = 50,000$. Gray lines indicate forced flow.

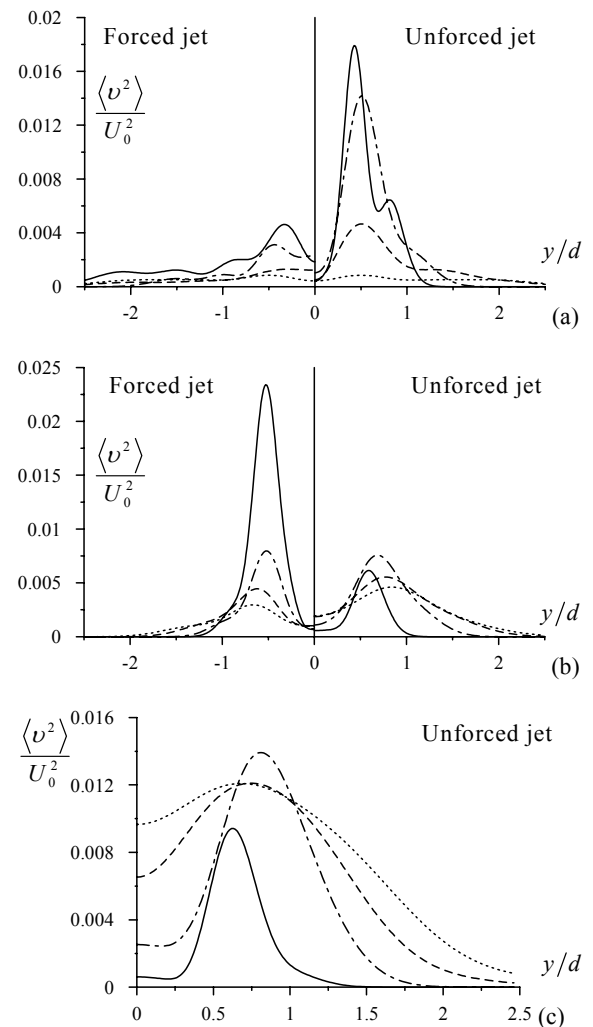


Figure 8: Distributions of the spanwise turbulent kinetic energy component at various cross-sections of slot jet. For captions see Figure 3.

Summarizing one can conclude that while forcing has no significant effect on the flows with $Re \geq 20,000$, while it strongly affects flows with $Re = 2,000$ and $Re = 10,000$ leading to considerably different regimes from the unforced cases. The forced flow regimes are characterized by significantly greater values of the second- and third-order moments in the initial region of the flow.

Terms of balance equations

The present section of the work is devoted to the estimation of the terms of the axial mean momentum and turbulent kinetic energy balance equations for the far field ($x/d = 6$) of the slot jet with relatively high Reynolds number, $Re = 20,000$.

The studied slot jet flows are described using a Cartesian coordinate system. The coordinates (x, y, z) denote the streamwise, spanwise, and cross-stream directions, respectively. Correspondingly, (U, V, W) and (u, v, w) are the streamwise, spanwise, and cross-stream components of the mean and fluctuating velocity.

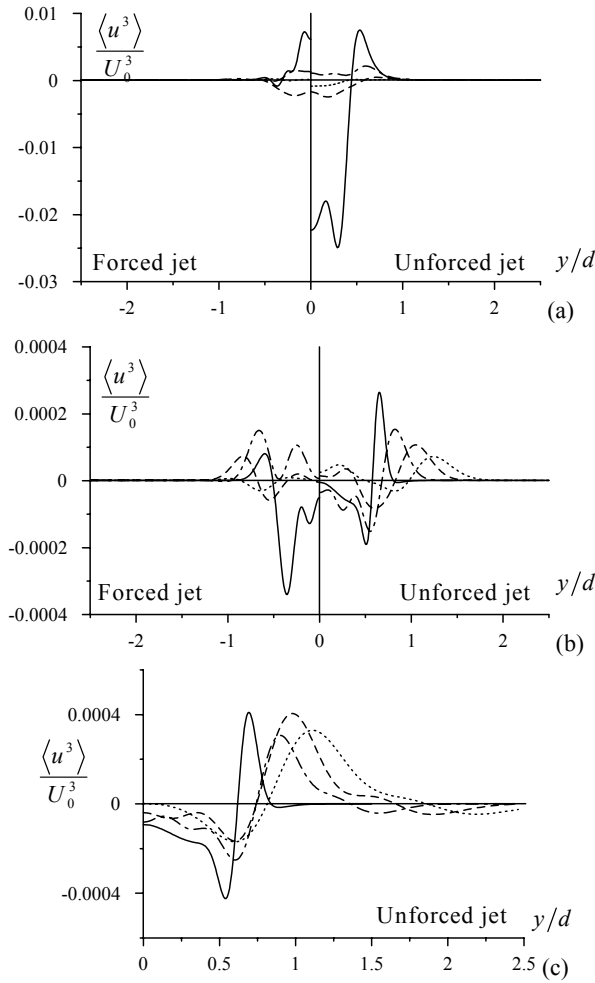


Figure 9: Distributions of the spanwise turbulent kinetic energy component at various cross-sections of slot jet. For captions see Figure 3.

The used 2D PIV approach does not allow to measure cross-stream velocity component, as well as spatial derivatives in the cross-stream direction. Basing on indirect evidence of flow quasi two-dimensionality concluded from the calculated spectra, the intensity of cross-stream velocity fluctuations w were assumed to be negligible in comparison to u and v . Also, DNS data on a fully developed channel flow by Kim et al. (1987) was used for evaluation of the cross-stream derivatives contribution to the balance equations.

Considering reflection symmetry for the central plane ($z = 0$) of the slot channel, the cross-stream mean velocity W and all moments containing odd power of cross-stream velocity fluctuations (but not their derivatives in z direction) can be assumed to be zero. Using these conditions for incompressible stationary flow, the axial mean momentum transport equation is given by (1):

$$-\left(V \frac{\partial U}{\partial y} + U \frac{\partial U}{\partial x}\right) - \left(\frac{\partial \langle uv \rangle}{\partial y} + \frac{\partial \langle u^2 \rangle}{\partial x} + \cancel{\frac{\partial \langle uw \rangle}{\partial z}}\right) - \frac{\partial P}{\rho \partial x} + \nu \left(\frac{\partial^2 U}{\partial x^2} + \frac{\partial^2 U}{\partial y^2} + \cancel{\frac{\partial^2 U}{\partial z^2}}\right) = 0 \quad (1)$$

Here, ρ denotes flow density, P is the mean pressure, ν is the kinematic viscosity and $\langle \rangle$ indicates ensemble averaging. The first and second bracketed terms in the left-hand side of equation (1) correspond to convection and turbulent diffusion, while the third and fourth bracketed terms correspond to transport by the mean pressure gradient and viscous diffusion, respectively. The turbulent kinetic energy (TKE) budget equation is given by (2):

$$A + D_r + D_p + D_v + P - \varepsilon = 0 \quad (2)$$

$$A = - \left(V \frac{\partial \langle q^2 \rangle}{\partial y} + U \frac{\partial \langle q^2 \rangle}{\partial x} \right) \quad (3)$$

$$D_r = - \left(\frac{\partial \langle q^2 v \rangle}{\partial y} + \frac{\partial \langle q^2 u \rangle}{\partial x} + \cancel{\frac{\partial \langle q^2 w \rangle}{\partial z}} \right) \quad (4)$$

$$D_p = \frac{1}{\rho} \left(\frac{\partial \langle p v \rangle}{\partial x} + \frac{\partial \langle p u \rangle}{\partial y} + \frac{\partial \langle p w \rangle}{\partial z} \right) \quad (5)$$

$$D_v = \nu \left(\frac{\partial^2 \langle q^2 \rangle}{\partial x^2} + \frac{\partial^2 \langle q^2 \rangle}{\partial y^2} + \cancel{\frac{\partial^2 \langle q^2 \rangle}{\partial z^2}} \right) \quad (6)$$

$$P = - \left(\langle u^2 \rangle \frac{\partial U}{\partial x} + \langle v^2 \rangle \frac{\partial V}{\partial y} + \langle w^2 \rangle \cancel{\frac{\partial W}{\partial z}} + \langle uv \rangle \left(\frac{\partial V}{\partial x} + \frac{\partial U}{\partial y} \right) \right) \quad (7)$$

Here, $q^2 = (u^2 + v^2)/2$ is the turbulent kinetic energy and the crossed terms in (1), (4), (6) and (7), according to the DNS data on channel flow, are considered to have a minor contribution to the balance equations.

The first and second terms on the left-hand side of (2) correspond to convection and turbulent diffusion. The third and fourth terms represent pressure and viscous diffusion. The fifth and sixth bracketed terms indicate shear production and the TKE dissipation rate.

In Figures 10a and b profiles of the second- and third-order moments are presented for $Re = 20,000$ at $x/d = 6$. One can notice that their magnitude is significantly lower in comparison to the well-known data on free plane or axisymmetric jets.

Distributions of the axial mean momentum transport equation terms are presented in Figure 11a. Transport by mean pressure gradient was found as a residual term of the equation. Calculated viscous diffusion has insignificant value (for both laminar and turbulent distributions of the mean velocity in the cross-stream direction) for the present cross-section and thus is omitted. It can be concluded, that mainly convection and mean pressure gradient contribute to the axial mean momentum transport for this cross-section.

For the TKE budget presented in Figure 11b similarly to the momentum transport, viscous diffusion was found to be negligible and is not plotted. The convection term in TKE budget is rather small and has maximum values about two times lower than magnitude of the pressure diffusion. Similarly to free shear flows, the production term has an off-axis peak, corresponding to the mixing layer. The dissipation was not measured directly from the velocity fields in the present work. Thus pressure diffusion and dissipation are presented together as the residual term.

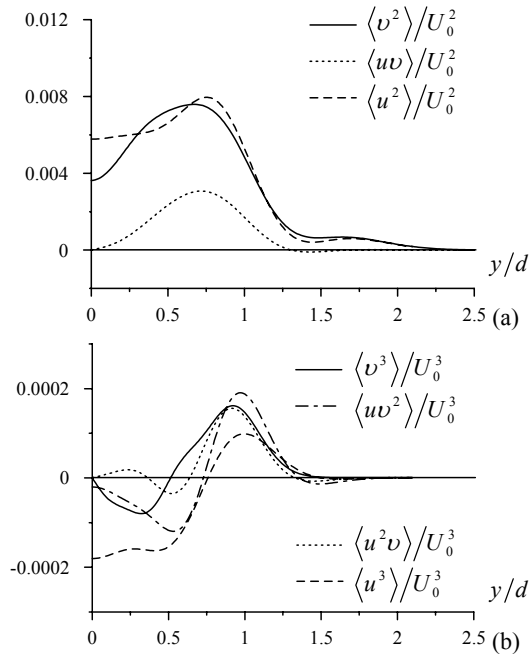


Figure 10: Profiles of the second- and third-order moments at $x/d=6$ cross-section for unforced slot jet with $Re = 20,000$. (a) Second-order and (b) third-order moments.

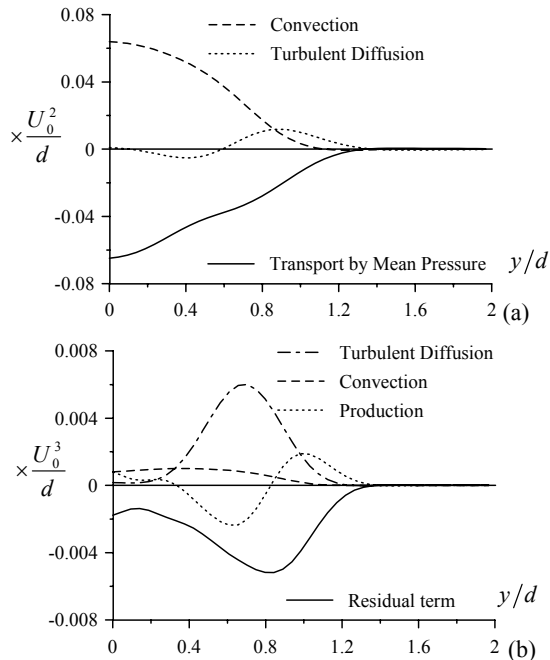


Figure 11: Normalized terms of balance equations for unforced slot jet at $Re = 20,000$, $x/d=6$ cross-section. (a) Axial mean momentum transport equation. (b) Turbulent kinetic energy budget.

CONCLUSIONS

Turbulent structure of a jet spreading in a narrow channel at various Re (from 500 up to 50,000) is studied experimentally by using 2D2C PIV. One-dimensional spatial spectra of velocity fluctuations were calculated for initial and far regions of the jet at $Re = 20,000$ and -3 and -1 slopes were clearly observed. Slope -3, corresponding to large-scale quasi 2D vortical structures, was at low wavenumbers region. An application of external low-amplitude forcing of inlet velocity led to enhancement of the large-scale vortices generation in the jet mixing layer and strongly affected near field of the jets at low and moderate Re numbers ($Re = 2,000$ and $10,000$) leading to substantially high values of the second- and third order moments.

For the studied flow at high $Re = 20,000$, terms of the mean momentum and turbulent kinetic energy budget equations were estimated for a far region of the jet. For the axial mean momentum, it was found that convection and mean pressure gradient are about six times greater than the turbulent transport and they mainly contribute to the balance equation. Contrary, for the TKE budget, convection was found to be rather small in comparison to the other terms: about two times lower than turbulent diffusion and about six times than the production term.

ACKNOWLEDGEMENTS

This work is supported by RAS and SB RAS integration research projects and by the RFBR foundation, grant N 07-08-00213.

REFERENCES

- Chu, V.H., and Baines, W.D., 1989, "Entrainment by a Buoyant Jet Between Confined Walls", *Journal of Hydraulic Engineering*, Vol.115, pp. 475-492.
- Dracos, T., Giger, M., and Jirka, G.H., 1992, "Plane Turbulent Jets in a Bounded Fluid Layer", *Journal of Fluid Mechanics*, Vol. 241, pp. 587-614.
- Gorin, A.V., Sikovsky, D.Ph., Nakoryakov, V.E., and Zhak, V.D., 1998, "Two-dimensional Turbulent Jet in a Hele-shaw Cell", *Proceedings, 7th International Symposium on Flow Modeling and Turbulence Measurements*, Tainan, Taiwan, pp. 269-279.
- Heinz, O.M., Ilyushin, B.B., and Markovich, D.M., 2004, "Application of a PDF's method for the statistical processing of experimental data", *Int. Journal of Heat and Fluid Flow*, Vol. 25, pp. 864-874.
- Kim, J., Moin, P. and Moser, R., 1987, "Turbulence Statistics in Fully Developed Channel Flow at the Low Reynolds Number. *Journal of Fluid Mechanics*, Vol. 177, pp. 133-166.
- Nakoryakov, V.E., Zhak, V.D, and Safonov, S.A., 1991, "Flow in a Hele-Shaw Cell at Large Velocities", *Russian Journal of Engineering Thermophysics*, Vol. 1, pp. 1-23.
- Pesci, A.I., Porter, M.A., and Goldstein, R.E., 2003, "Inertially Driven Buckling and Overturning of Jets in a Hele-Shaw Cell. *Physical Review E*, Vol. 68, 056305.